Integration of a drying and pyrolysis system in a green biorefinery

biochar product quality and impacts on the overall energy balance and climate footprint

Ravenni, G.; Thomsen, T. P.; Smith, A. M.; Ambye-Jensen, M.; Rohde-Nielsen, K. T.; Henriksen, Ulrik B.

Published in:
Biomass Conversion and Biorefinery

DOI:
10.1007/s13399-023-04877-4

Publication date:
2023

Document Version
Publisher's PDF, also known as Version of record

Biomass Conversion and Biorefinery
https://doi.org/10.1007/s13399-023-04877-4

ORIGINAL ARTICLE

Integration of a drying and pyrolysis system in a green biorefinery: biochar product quality and impacts on the overall energy balance and climate footprint

G. Ravenni[1] · T. P. Thomsen[2] · A. M. Smith[3] · M. Ambye-Jensen[3] · K. T. Rohde-Nielsen[4] · Ulrik B. Henriksen[1]

Received: 13 April 2023 / Revised: 24 August 2023 / Accepted: 7 September 2023

Abstract

Green biorefineries can support the reduction of soybeans imports to Europe, by producing protein-rich animal feed from alternative feedstock such as perennial grass and legume species. Once the protein-rich green juice is extracted, a fiber-rich pulp is left as a residue. This work investigates the thermochemical processing of the pulp via pyrolysis as an option to improve the energy balance and climate footprint of a green biorefinery, by producing non-fossil energy and a high-value biochar product. Laboratory-scale pyrolysis and biochar activation were carried out on pulp samples obtained from different perennial species, different pressing method, and maturity at harvest. The results highlighted the importance of the activation stage to obtain a porous biochar, potentially suitable as animal feed additive. The effects on the overall energy balance and climate impact of the system following the integration of pulp drying and pyrolysis, plus a possible activation step for the biochar, were evaluated with a techno-environmental assessment. The pulp sample composition had only limited influence on the climate impact potentials identified. In all cases, it was found that the integration of a combined drying-pyrolysis-activation system in the green biorefinery may provide substantial additional climate benefits but also that the magnitude of these is strongly dependent on the substitution use-value of the energy products.

Keywords Green biorefinery · Pyrolysis · Biochar · Steam activation · Climate impact

Highlights
- The integration of a pyrolysis system in a green biorefinery was investigated.
- Steam activation was decisive to obtain porous biochars from residual pulp.
- Feedstock lower in minerals achieved a higher porosity with lower carbon burn-off.
- A techno-environmental assessment revealed significant potential climate benefits.

✉ G. Ravenni
grav@kt.dtu.dk

[1] Department of Chemical and Biochemical Engineering, CHEC center, Technical University of Denmark (DTU), Søltofts Plads 228A, 2800 Kgs. Lyngby, Denmark

[2] Department of People and Technology (IMT), Roskilde University (RUC), Universitetsvej 1, 4000 Roskilde, Denmark

[3] Biological and Chemical Engineering, Centre for Integrated Biorefining, Aarhus University Viborg, Blichers Allé 20, 8830 Tjele, Denmark

[4] AquaGreen ApS, Risø Huse 50, 4000 Roskilde, Denmark

1 Introduction

Intensive animal husbandry in northern Europe brings about a requirement to import protein-rich soy for use as animal feed. On average, 16 million tons of soybeans and 29 million tons of soybean cake were imported per year in Europe for the period 2009–2013 [1]. For intensive livestock producing countries such as Denmark, there is a desire to increase domestic feed protein supply to improve the self-sufficiency of the industry [2]. Processed protein-rich perennial grass is emerging as an attractive option in Denmark due to the potential for increased production as well as the beneficial effects of perennial grasses cultivation, including mitigation of nutrient leaching, reduced pesticide use, and soil protection from erosion [3]. Processing of protein-rich perennial species in green biorefineries can support the production of protein feed from indigenous grasses and legumes such as alfalfa, clover, and ryegrass [1]. The initial processing step in a green biorefinery extracts both sugars and proteins through maceration and pressing of biomass, forming a protein-rich green

Published online: 25 September 2023

juice and leaving a fibrous press cake with a moisture content of 60–70%, known as the pulp. The juice undergoes heat treatment and further processing to produce feed suitable for monogastric animals. To date, the pulp can either be used as anaerobic digestion feedstock or ensiled and used for ruminant feed. However, large-scale protein production would likely exceed ruminant feed demand, offering the opportunity to use this feedstock for other applications.

In this study, it is proposed that a combined drying and pyrolysis system is integrated in the green biorefinery process, providing a route to extract energy from the pulp to heat and dry the protein product, while producing valuable biochar. Grass-derived biomass is rarely considered as a feedstock for pyrolysis and biochar production, and there are only few studies available on the topic [4, 5]. However, in this context, the integration of drying and pyrolysis system in the biorefinery represents an attractive option in terms of overall energy efficiency. Moreover, biochar production represents a waste management solution that can improve the resource circularity of the biorefinery as well as reduce the overall climate intensity of the system to climate neutral or even climate negative [6, 7]. Biochar can find multiple uses for soil amendment, environmental management, and carbon sequestration [8]. There are also many emerging applications of biochar in an agricultural context including bulking agent for windrow composting [9], additive for anaerobic digestion [10], and bedding and feed additive in livestock farming [11, 12]. In the context of a green biorefinery producing protein-rich animal feed, the use of biochar as feed additive is a desirable option, which could also benefit the biorefinery climate impact by providing an indirect route for carbon sequestration [13] via pyrogenic carbon capture and storage (PyCCS) [14]. The use of charcoal in animal feed is documented since antiquity, and the use of activated carbon and charcoal for this application has been object of scientific research particularly in the last decade, reporting several benefits of mixing biochar with feed. The mechanisms behind the several beneficial effects of adding charcoal in animal feed are not yet completely understood, but biochar has been shown to improve the nutrient intake efficacy, adsorb toxins and pathogens and generally improve animal health [11]. The use of vegetable charcoal as feed additive is authorized in the European Union, and included in the European Commission Regulation 575/2011 [15]. The European Biochar Certificate provides dedicated guidelines for the production of feed additive from biochar, and since 2020, all types of pure plant biomasses are approved for the production of EBC-Feed biochar according to the EBC feedstock list [16]. Previous studies show that the most beneficial effects of biochar as feed additive are achieved when biochar has a developed porosity and a relatively large specific surface area: these properties, together with the surface chemistry of the material, are known to play an important role in determining the adsorption capacity of biochar towards a variety of substances [11, 12].

The production of porous carbons from agricultural residues has been investigated in previous works with the purpose to find sustainable precursors for the production of carbon adsorbents [17], which nowadays are mainly obtained from fossil sources including bituminous coal, peat, petroleum, pitch and polymers, and from coconut shells [18, 19]. The methods used in the production of porous carbons are chemical and physical activation. Chemical activation involves the impregnation of the biomass with chemicals such as KOH, H_3PO_4, and $ZnCl_2$. Considering the target application of biochar as feed additive, the chemical activation method is potentially problematic; therefore, the focus in the present work is on steam activation, which is known to increase significantly the porosity of char produced via pyrolysis, and to induce the formation of larger pores compared with CO_2 activation [20, 21]. Indeed, micropores (with a pore diameter < 2 nm) may not be effective in adsorbing high molecular weight substances or bacterial pathogens relevant for animal digestion. Galvano and colleagues [22] found that highly microporous activated carbon had lower adsorption capacities for aflatoxins due to the difficult diffusion of these toxins into the pore structure. This was also the case for other investigated toxic compounds such as pesticides, PCBs, dioxins, or pathogens, as was demonstrated when highly activated biochar did not reduce the toxic effects of aflatoxin in chickens more strongly than non-activated biochar [23].

In addition to providing a biochar product, the integration of pyrolysis within the green biorefinery is also expected to positively affect the overall energy balance. To process the green juice and precipitate proteins, there is an inherent requirement for heat, and pulp could be used as feedstock for in-house energy production via process integration with various energy technologies [24]. Integrated energy supply from by-product utilization has been investigated previously and may increase both the energy-efficiency of the biorefinery as well as potentially improve the net value production and environmental impacts [25–27]. The hypothesis of this work is that the combustion of pyrolysis volatiles would generate enough energy to dry the incoming pulp and sustain the pulp pyrolysis process, possibly including a biochar activation step. Process waste heat could then be used to precipitate proteins from the green juice. This solution is based on a system combining superheated steam drying and thermal pyrolysis, a technology developed by the Danish company AquaGreen ApS, in collaboration with DTU Chemical Engineering. The AquaGreen combined system has been found to be a highly energy-efficient process for treatment of very wet substrates [28, 29].

The purpose of this work is to investigate the integration of a pyrolysis system into a green biorefinery concept, moving from the study of the production of pulp biochar for use as feed additive, to an assessment of the potential energy recovery and climate impact effects of the proposed system integration. The novelty of this work resides in the consideration of grass and legume pulp as biochar feedstock, and in the combined approach of biochar product assessment together with energy and climate considerations. The properties of biochars produced via laboratory-scale pyrolysis and steam activation from different types of pulp are assessed and the influences of grass species, harvesting season and process parameters are evaluated for the production of biochar feed additive. Moreover, the energy recovery achieved through the system integration of pyrolysis in the green biorefinery is evaluated in terms of both energy efficiency and climate impact, including the potential carbon-sink effect provided by biochar.

2 Material and methods

2.1 Feedstock

Pulp samples were obtained from different grass and legume perennial species grown and harvested in Denmark: clover (*Trifolium*), alfalfa (*Medicago sativa*), and ryegrass (*Lolium*). The pulp samples were produced at the pilot-scale green biorefinery at Aarhus University [27] in spring 2020, and were treated either by a single stage pressing (1SP) or a two stage pressing (2SP) in the twin screw press that extracts the juice. In other words, the grass pulp has had its protein rich juice extracted by either a single or a double pressing in a screw press. Two further clover and alfalfa samples were collected from a later harvest (November 2020). Both these samples were processed at the same pilot biorefinery as the previous ones, and pressed twice to extract the juice. Pulp samples were frozen after processing and the average moisture content measured on the frozen samples was 70 ± 4 wt%. This was measured after drying the samples for 12 h in an oven at 105 °C. All further experiments and analyses were carried out using the dry pulp samples. Pine wood chips were included in this study as a reference feedstock. Moreover, a biochar product commercialized as feed additive (CFA) was acquired for comparison with the produced biochars. According to the producer, CFA is produced specifically for pigs from a mix of wood, husks and fruit stones.

2.2 Biochar production and activation

The pulp samples were pyrolyzed in a laboratory-scale batch pyrolysis oven. Three subsamples of each biomass type were arranged in a sealed pyrolysis reactor ($31 \times 10 \times 16$ cm) and flushed for about 10 min with N_2 (1.5 l/min) at room temperature. The reactor was then heated to 600 °C with a heating rate of 10 °C/min, and the reactor was retained at 600 °C for 40 min. A total of 25 to 30 g of biomass was pyrolyzed in each batch. The steam activation of char samples was carried out using a cylindrical reactor (12 cm diameter, 13.5 cm height), with a crucible capable of holding about 2 g of biochar. The reactor was electrically heated up to the desired temperature under N_2. When the temperature set point was reached, the N_2 flow was stopped and a steam flow of 1 kg/h was started. After 30 min, the supply to the reactor was switched back to N_2 and maintained to allow the sample to cool down. The steam activation was carried out at 650 °C, and the char samples were weighed before and after the treatment. The steam activation was repeated twice on each biochar to verify the repeatability of the results in terms of mass loss and final specific surface area.

2.3 Characterization of feedstock and biochar

The proximate composition of the biomass samples was determined using the results of the pyrolysis runs to assess the content of volatiles, while the ash content was assessed with incineration in air at 550 °C for 12 h. The fixed carbon content was calculated by difference. The elemental composition of the dried pulp and of the biochar samples (CHN) was determined with an elemental analyzer (EA3000, Eurovector, Italy), as the average over four measurements for each sample.

The elemental analysis was repeated also on the activated chars. The results were combined with the compositional values obtained on the dry pulp and after the pyrolysis step, as well as the mass loss after the pyrolysis and activation treatments. These values were used to calculate the carbon loss (C burn-off) in both steps. In Eq. 1, C_{initial} is the amount of carbon in the dry biomass, while C_{final} refers to the amount of carbon contained in the samples after pyrolysis and after activation, and is the average of two repetitions.

$$\text{Cburn} - \text{off}[\%] = \frac{C_{\text{initial}}[g] - C_{\text{final}}[g]}{C_{\text{initial}}[g]} \times 100 \quad (1)$$

Fiber analysis was undertaken to determine the content of cellulose, hemicellulose, and lignin in the pulp samples. The analysis was done using the Van Soest fiber analysis method, which determines the main fibers present via sequential sample extraction. Neutral detergent fiber (NDF) and acid detergent fiber (ADF) were determined using Fibertech 2010 (Foss Analytics, DK), using 0.5 g of sample, alpha amylase to degrade the starch to soluble sugar, and sodium lauryl sulphate and ethylenediaminetetraacetic acid (EDTA) as the detergent. The initial extraction removes the neutral detergent solubles (NDS) which include, protein, starch,

sugars, organic acids, and pectin, leaving the NDF (hemicellulose, cellulose, lignin, and ash). The NDF was subsequently extracted using cetyltrimethylammonium bromide in 1 mol sulphuric acid to remove the acid detergent solubles (ADS) which is primarily hemicellose, leaving the ADF, which consists of cellulose, lignin, and ash. Cellulose and lignin content was then determined using the acid detergent lignin (ADL) method, where 0.5 g of sample was soaked in 72% sulphuric acid for 48 h, filtered, dried, and weighed. The lignin content was then calculated by ashing the sample at 550 °C and subtracting the ash from the remaining fiber mass. The analysis was done in triplicate.

The surface area and porosity of the produced biochars were assessed with N_2 adsorption at 77 K. The specific surface area of the chars was calculated using the Brunauer–Emmett–Teller (BET) method. For activated biochars, the surface area was measured on both repetitions, and the average was calculated. The pore volume and pore size distribution was obtained with quenched solid density functional theory (QSDFT) on the adsorption branch, assuming pores were slit and cylindrical. The structure of the biochars surface was also evaluated with a scanning electron microscope (SEM) (Prisma E, ThermoScientific). The composition of the inorganic fraction of the different pulp samples was carried out with inductively coupled plasma–optical emission spectrometry (ICP-OES). Before the analysis, around 0.3 g of sample has been microwave digested using the USEPA 3051 method with 9 ml 65% HNO_3, 3 ml 30% HCl, and 4 ml 30% H_2O_2.

The thermal degradation behavior of biochars was analyzed by thermogravimetric analysis (TGA) (TGA/DSC 3 + , Mettler Toledo, USA). Five milligrams of sample were heated under 50 ml/min air in 30 µl alumina crucibles from 40 to 900 °C at 10 °C /min heating rate. The first derivative of the weight loss curves was calculated. Derivative thermogravimetry (DTG) gives the rate of weight changes against temperature and is used to simplify reading the thermogram, giving peaks where the oxidation (combustion) of compounds of different thermal stability occur, with the peak area proportional to the carbon present. DTG curves can be found in the supplementary material. The recalcitrance index (R_{50}) of the biochar was also obtained from the weight loss data. R_{50} is calculated as the ratio between the temperature at which 50% of the biochar total mass is lost (T_{50}) and the T_{50} for a graphite reference (886 °C) as shown below.

$$R_{50}\text{biochar} = \frac{T_{50}\text{Biochar}}{T_{50}\text{Graphite}} \quad (2)$$

The R_{50} was calculated as in Harvey and colleagues [30], based on the hypothesis that biochars with higher environmental recalcitrance, and therefore, higher carbon sequestration potentials are increasingly resistant to oxidation and therefore will require higher energy inputs to mineralize a unit mass of biochar carbon to CO_2. R_{50} values were used alongside H/C ratios to evaluate the theoretical stability of the carbon in the biochar.

2.4 Techno-environmental assessment of the potential climate impact from energy production and carbon sink effects

The assessment of biochar production was complemented by the analysis of the potential energy recovery in the integrated system encompassing the green biorefinery and thermal pyrolysis of the pulp residue. The investigated system also models the inclusion of biochar steam activation in the AquaGreen combined superheated steam drying and pyrolysis. Drying, pyrolysis, and biochar activation are carried out in continuous auger reactors. The system is illustrated in Fig. 1, including expected integration points between the thermal processes and the green biorefinery processes (A and B points) and products expected primarily for export (C points).

Energy and mass flows and potential climate effects were calculated per ton of pulp treated in the proposed system. The calculations were performed following the method described in Liu et al. [31], on the whole system and three subsystems, as illustrated with dotted, red squares in Fig. 1.

It was estimated how much of the energy in the pyrolysis gas is required to drive the drying and pyrolysis of the feedstock as well as the biochar activation step, and how this varies with the different pulp substrates and moisture contents. The energy- and mass balances for the pyrolysis were predominantly based on the laboratory-scale pyrolysis and activation, feedstock, and biochar characterization results from this study. In addition, the higher heating value (HHV) of dry pulp and biochar samples was determined in a Parr 6300 Bomb Calorimeter with an oxygen supply at 40 bar using 0.5–0.8 g samples. The analysis was done in triplicates. The calculations are based on the following parameters:

- Global specific heat capacity of water, biomass dry matter, biochar, bio-oil, and non-condensable gases: 4.19 kJ/kg•K, 2.0 kJ/kg•K, 1.0 kJ/kg•K, 1.47 kJ/kg•K, and 1.14 kJ/kg•K [32–34]. For pyrolysis gas, an average specific heat capacity of 1.3 kJ/kg•K is used, calculated as the average of the values for condensable and non-condensable constituents thereby assuming a 50/50 split on mass. The differences among the values are limited, and the impact of the assumption is therefore expected to be limited as well.
- Latent heat of vaporization of water at 100 °C and atmospheric pressure of 2.26 kJ kg^{-1} [35].

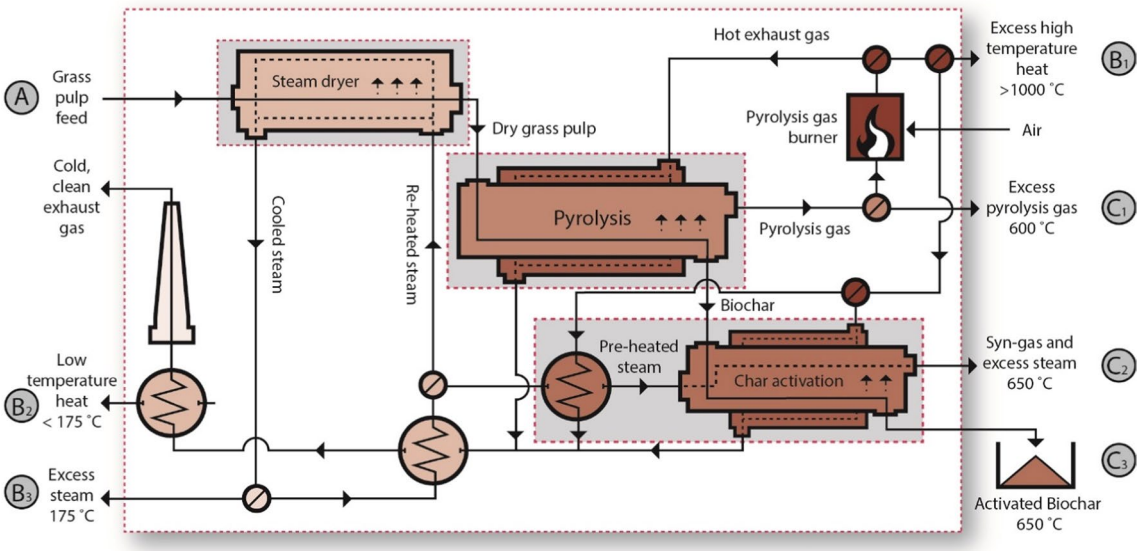

Fig. 1 Process diagram showing the thermal system consisting of steam drying, pyrolysis, and biochar steam activation. The integration to the green biorefinery is through feed intake (A) and potentially the products: excess high temperature heat (B1), low temperature heat (B2), and excess steam (B3). In situations with a high energy surplus, some of this energy may also be exported out of the biorefinery together with the other products: excess pyrolysis gas (C1), syn-gas and excess steam mixture (C2), and activated biochar (C3). Red dotted squares indicate boundaries for energy- and mass balance

- Ideal heat exchangers in all stages, but a net loss of sensible heat from machinery surfaces to surroundings of 5% of energy input in the low temperature processes (drying) and 10% in the high temperature processes (pyrolysis and steam activation). Size of heat losses to surroundings is based on the developing company's experience from previous pilot scale campaigns.
- Dryer inlet and outlet temperatures of the grass pulp: 20 °C and 120 °C, respectively.
- Dryer inlet and outlet temperatures of superheated steam: 250 °C and 175 °C, respectively.
- Pyrolysis reactor inlet and outlet temperatures: 120 °C and 600 °C, respectively.
- Steam activation step of biochar maintained at 650 °C, through steam pre-heating and external heating of reactor. Steam activation inlet and outlet temperatures are both 650 °C. A steam/total carbon ratio of 5 (molar basis) was assumed for all char activation processes, based on the setup used for the laboratory scale activation experiments.
- Energy requirements for slightly endothermic reactions in the pyrolysis process: 200 kJ/kg dry matter pyrolyzed [36].
- All mass lost during steam activation is assumed to be carbon, and the sum of the energy requirements for the highly endothermic reactions in the steam activation process is assumed to be completely dominated by the reaction $C + H2O \leftrightarrow CO + H2$, requiring 131 kJ/mol carbon converted [37].
- Use of the activation gas from char activation is assumed to include moisture reduction by cooling and condensation of the gas prior to high-temperature combustion. Low temperature heat is recovered from the cooling and condensation step.
- A carbon stability of at least 70% after 100 years is assumed for all samples, based on the BC_{+100} approach. This approach uses the H/C ratio as a proxy for carbon stabilization induced to a large extent by aromatic condensation of the carbon in the biochar. $BC_{+100} = 0.7$ results in 70% carbon stability after 100 years which is a conservative estimate, based on a statistical analysis conducted by IBI in 2013 and valid for biochars with $H/C \leq 0.4$ [38].
- Potential climate change impact value of the energy production is based on data from the BioGrace II database standard calculation values [39], except for the value of Danish marginal district heating which is modeled as described in Thomsen [40], using predominantly marginal electricity in large scale heat pumps [41] and combustion of biomass, but supplemented by other minor sources. This model uses data from the Ecoinvent database 3.7.1 (Substitution, consequential, long-term data) [42] as well as Easetech official 2020–01 v2 database for selected combustion processes, all by Turconi et al.[43].

The following climate change impact values are used in the present work:

- Replacing natural gas (EU-mix): 66.0 g $CO_{2\text{-eq}}$ per MJ [39]
- Replacing hard coal: 112.2 g $CO_{2\text{-eq}}$ per MJ [39]
- Replacing marginal, Danish district heating (near future): 10.4 g $CO_{2\text{-eq}}$ per MJ using IPCC's impact assessment method from 2013: Global Warming Potential, 100 years, Long term without climate carbon feedback as also applied in Thomsen 2021 [40].

It was assumed that all heat requirements in the process are provided by heat and chemical energy available in the pyrolysis gas. The primary heat requirements in the process were calculated as (i) heating of the biomass including moisture to 120 °C (for drying) and water evaporation with subsequent heating of the produced steam to an average steam outlet temperature of 175 °C, (ii) heating of the dry biomass to 400 °C (for pyrolysis) and release of pyrolysis gases (slightly net endothermic set of reactions), (iii) heating of condensable and non-condensable parts of the pyrolysis gas as well as the biochar to 600 °C, (iv) steam pre-heating for biochar activation at 650 °C and supplying additional energy for heating biochar to 650 °C and for endothermic gasification reactions, and (v) heat energy in products and loss of heat from plant surfaces.

3 Results and discussion

3.1 Characterization of pulp biomass samples and pyrolysis biochars

The proximate composition of the pulp samples and the reference biomass (pine chips) is reported in Table 1. The char yields after pyrolysis correspond to the sum of fixed carbon and ash fractions. The thermal decomposition of the pulp samples during pyrolysis was similar across all types of pulps, with char yields varying between 26 and 32%, while the pine chips reference exhibited a char yield of 24%. The differences in char yields appeared to be predominantly due to the ash content of the different samples, with pine chips showing a much lower ash content (0.2%) in comparison with the pulp samples, all in the range 3–9%. Interestingly, among the pulp samples, 2SP samples showed a slightly lower ash content in comparison with the 1SP: this is an expected effect of the double pressing, which extracts more protein, sugar, as well as water-soluble minerals from the feedstock. To account for this varying ash contents, the char yield was also calculated on an ash-free basis, which gave yields of 24–25% (dry- and ash-free basis) for all the samples, including pine chips. The contents of the main inorganic species present in the pulp samples are reported in Table 2, and the results of the Van Soest fiber analysis on the pulp samples are summarized in Table 3.

Potassium (K) and calcium (Ca) were the most abundant elements detected in the samples, followed by phosphorus (S), sulfur (S), and silicium (Si). The main differences among the samples were seen in the content of K, S, and Si, most abundant in clover 1SP, 2SP, and in rye 1SP. In contrast, the two samples from the November harvest showed the highest content of Ca and a low amount of K compared with the samples from an earlier harvest. The results on the content of cellulose, hemicellulose, and lignin clearly indicate that the November harvested alfalfa and clover have the highest lignin content. The change in the ash composition as well as the higher lignin content can be ascribed to the later stage of the maturation process. The higher lignin can also explain the slightly higher char yields obtained for these samples, as its understood that lignin contributes to a larger proportion of the biochar fraction than say cellulose [44, 45].

Table 4 reports the elemental composition of the pulp samples and references pine chips and CFA. The elemental analysis carried out on the biochars, after the pyrolysis step showed that all the grass and herbaceous biochars had a carbon content of at least 60%. Pine chips had the highest carbon content of 90%; however, it is worth

Table 1 Proximate composition of pulp samples and pine chips reference (dry basis). *Calculated by difference

	Dry basis (wt%)				Dry- and ash-free basis (wt%)
	Volatiles	Ash	Fixed carbon*	Char yield	Char yield
Clover 1SP	68.5 ± 0.1	8.8 ± 0.5	22.7	31.5	24.8
Clover 2 SP	69.2 ± 0.1	8.1 ± 0.7	22.7	30.8	24.7
Rye 1SP	71.4 ± 0.7	5.4 ± 0.1	23.2	28.6	24.4
Rye 2SP	74.0 ± 0.6	3.0 ± 0.2	23.0	26.0	23.7
Alfalfa 2SP	70.6 ± 0.6	5.7 ± 0.8	23.7	29.4	25.1
Clover Nov20 2SP	69.1 ± 0.3	6.3 ± 0.2	24.6	30.9	25.9
Alfalfa Nov20 2SP	67.5 ± 0.5	7.6 ± 0.7	24.9	32.5	27.1
Pine chips	75.6 ± 0.2	0.2 ± 0.1	24.2	24.4	24.2

Table 2 Contents of main inorganic elements in the pulp samples measured by ICP-OES

	Dry basis [mg/kg]					
	K	**Ca**	**P**	**Mg**	**S**	**Si**
Clover 1SP	18682 ± 190	4241 ± 31	2158 ± 10	1090 ± 11	2225 ± 15	1360 ± 18
Clover 2 SP	26676 ± 2 41	4344 ± 39	3819 ± 36	1500 ± 21	2326 ± 38	1292 ± 9
Rye 1SP	20374 ± 407	3464 ± 25	2927 ± 21	1347 ± 20	2253 ± 18	858 ± 14
Rye 2SP	10788 ± 198	3118 ± 34	2077 ± 9	1019 ± 15	1955 ± 25	975 ± 18
Alfalfa 2SP	12831 ± 146	6622 ± 106	2047 ± 27	932 ± 2	1475 ± 22	790 ± 5
Clover Nov20 2 SP	10956 ± 12	7187 ± 79	1832 ± 25	1233 ± 10	1405 ± 21	1596 ± 8
Alfalfa Nov20 2 SP	8288 ± 108	9459 ± 185	1316 ± 16	909 ± 3	1297 ± 17	510 ± 9

Table 3 Fiber analysis of pulp samples via Van Soest method

Dry basis (wt%)				
	Extractives	**Hemicellulose**	**Cellulose**	**Lignin**
Clover 1SP	26.1 ± 0.3	31.3 ± 0.5	28.1 ± 2.3	5.8 ± 1.5
Clover 2 SP	23.5 ± 1.4	34.0 ± 0.6	30.2 ± 0.7	4.1 ± 0.6
Rye 1SP	25.4 ± 0.7	35.9 ± 0.2	31.4 ± 0.6	1.7 ± 0.8
Rye 2SP	19.2 ± 0.3	41.3 ± 0.2	33.1 ± 2.4	3.6 ± 2.3
Alfalfa 2SP	25.6 ± 0.6	25.8 ± 0.3	33.5 ± 0.4	9.6 ± 0.4
Clover Nov20 2SP	21.3 ± 0.1	29.1 ± 0.3	33.2 ± 0.2	10.0 ± 0.1
Alfalfa Nov20 2SP	21.6 ± 0.7	21.9 ± 0.8	35.6 ± 1.6	13.4 ± 1.5

Table 4 Elemental composition of biochars. *Calculated by difference, using ash content values reported in Table 1

Dry basis (wt%)				
	Carbon	Hydrogen	Nitrogen	Oxygen*
Clover 1SP	60.4 ± 2.2	2.0 ± 0.1	5.1 ± 1.6	4.5
Clover 2 SP	64.2 ± 1.9	2.2 ± 0.2	2.9 ± 0.6	4.4
Rye 1SP	62.4 ± 0.8	1.8 ± 0.0	2.0 ± 0.1	14.5
Rye 2SP	70.2 ± 3.0	2.1 ± 0.1	2.6 ± 0.1	13.4
Alfalfa 2SP	62.8 ± 3.7	1.9 ± 0.0	7.3 ± 1.4	8.5
Clover Nov20 2SP	70.2 ± 2.0	1.6 ± 0.0	1.2 ± 0.2	5.8
Alfalfa Nov20 2SP	74.0 ± 3.0	1.7 ± 0.1	1.1 ± 0.2	0.1
Pine chips	89.8 ± 1.3	2.4 ± 0.0	1.1 ± 0.3	6.0
CFA	44.6 ± 1.2	1.1 ± 0.1	0.6 ± 0.6	31.3

acknowledging that this sample had a low ash content, and if the grass and herbaceous chars are adjusted to a dry- and ash free basis, similarly, high carbon contents are obtained, between 77 and 96%. A notable exception to this is the CFA, the commercial biochar product, containing around 45% carbon, notably lower than the other samples despite having 22% ash.

Table 5 Specific surface area and porosity values for chars after pyrolysis and after the additional steam activation step. BET results of activated biochars are the average of two activated samples. DFT pore volume was calculated only on the first measurement, given the good agreement among repetitions. n.a. = not assessed

	Pyrolysis char		Pyrolysis + steam activation	
	BET	DFT	BET	DFT
	(m^2/g)	(cc/g)	(m^2/g)	(cc/g)
Clover 1SP	0.98	0.0018	119	0.0505
Clover 2SP	1.17	0.0023	317	0.1262
Rye 1SP	0.89	0.0024	421	0.1693
Rye 2SP	1.94	0.0034	369	0.1479
Alfalfa 2SP	1.36	0.0034	366	0.1622
Pine chips	450	0.1762	519	0.1963
CFA	64.8	0.0611	n.a	n.a
Clover Nov20 2SP	1.33	n.a	316	0.142
Alfalfa Nov20 2SP	1.17	n.a	362	0.2011

3.2 Steam activation of biochars

After pyrolysis, all the pulp-derived biochars were found to have a very low specific surface area (below 2 m^2/g) and pore volume (below 10 mm^3/g) (Table 5). These values are strikingly low when compared with values reported in literature for grass-derived biochars [4, 46]. This could be ascribed to the grass pressing process which might have caused structural modifications to the feedstock. The pine chips char on the other hand showed a much higher specific surface area and pore volume (450 m^2/g, 200 mm^3/g), this time in good agreement with values reported in literature [47, 48]: because the pyrolysis process was identical for all samples, such large difference was probably caused by the feedstock properties. The commercial feed product showed a lower surface area compared with the pine chips, but still significantly higher than the pulp biochars (64.8 m^2/g). In order to verify whether it was possible to achieve a better surface structure for the pulp biochars without an activation step, but only tuning the pyrolysis temperature, the influence of the pyrolysis temperature on the specific surface area

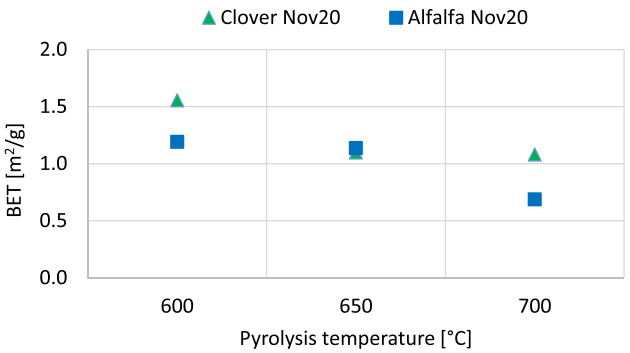

Fig. 2 Evolution of specific surface area of char samples produced at different pyrolysis temperature

was investigated on two samples. The clover and alfalfa harvested in November were pyrolyzed at 650 °C and 700 °C. The results on the specific surface area over the tested temperatures are reported in Fig. 2, and showed that increasing the pyrolysis temperature did not yield higher surface area, but instead seemed to have a slightly detrimental effect. The surface area of biochar is known to increase with increasing pyrolysis temperature due to the releasing of volatiles up to 800–900°C, while at higher temperatures the surface area may decrease again due to shrinking of the solid matrix, pore widening and coalescence as well as melting of ash, all leading to a reduction of the microporosity [48–50].

Despite the pressing process and the very low measured values for the specific surface area of pulp-derived biochars, SEM images revealed that even 2SP pyrolysis biochars exhibited a fibrous macrostructure, with visible xylems and pores (Fig. 3). The presence of these structures, together with the relatively high carbon content of the pyrolysis chars, suggested a good potential for improving the surface area by steam activation. Indeed, the channels and pores observed in the biochars can favor the diffusion of steam within the biochar particles, facilitating the surface area development via steam reforming reactions.

The steam activation treatment was performed in duplicate on the biochar samples. The mass loss was similar for all samples in both trials, with an average standard deviation of 5%. Consistently, the steam-activated duplicates were also found to have similar specific surface area, with an average standard deviation of 2%: the average BET specific surface area over the two repetitions is reported for all samples in Table 5. Given the good agreement among repetitions, the pore volume was calculated only on the first measurement for a qualitative assessment. Overall, results showed that steam activation had a dramatic effect on the porosity of all pulp biochars, in most cases achieving a final specific surface area well above 300 m^2/g. Interestingly, pine chips biochar did not benefit as much from the activation process but nevertheless achieved the highest surface area after activation (519 m^2/g).

The difference in the surface area measured before and after steam activation is a consequence of the C burn-off from the surface and subsequent creation of new pores and enlargement of the pores already present on the surface. However, such a large difference in specific surface area is also caused by the measurement method, which is influenced by the change in the pore size distribution on the biochars with activation. The surface of pyrolysis chars is known to be highly microporous (rich in pores smaller than < 2 nm), and the smaller pores are not accessible to N_2: this can lead to an underestimation of the specific surface area of pyrolysis chars. On the other hand, the steam activation makes the surface more accessible to the N_2 probe gas, and consequently its measurement via N_2 adsorption more accurate [51]. The much higher specific surface area measured on the activated samples clearly indicates a more open surface, potentially much more permeable to adsorb molecules such as toxins and other contaminants.

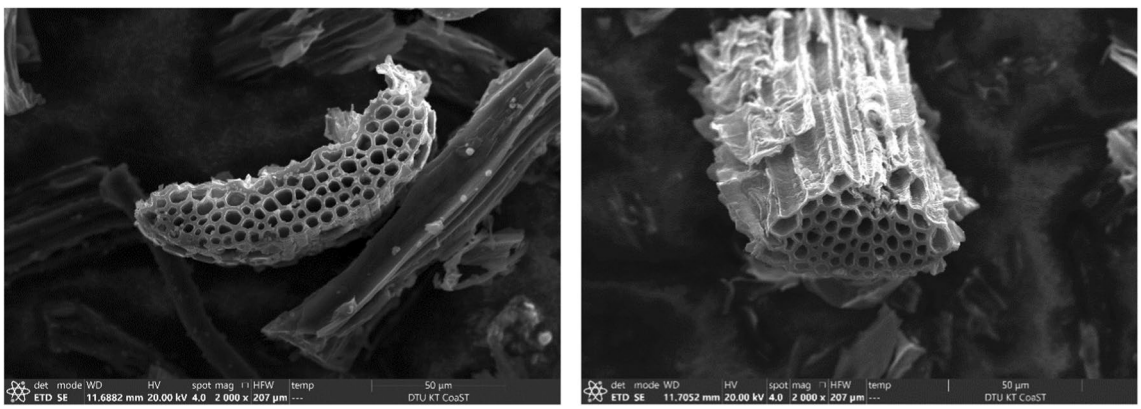

Fig. 3 SEM images of pyrolyzed fiber pulp: clover 2SP (left) and alfalfa 2SP (right)

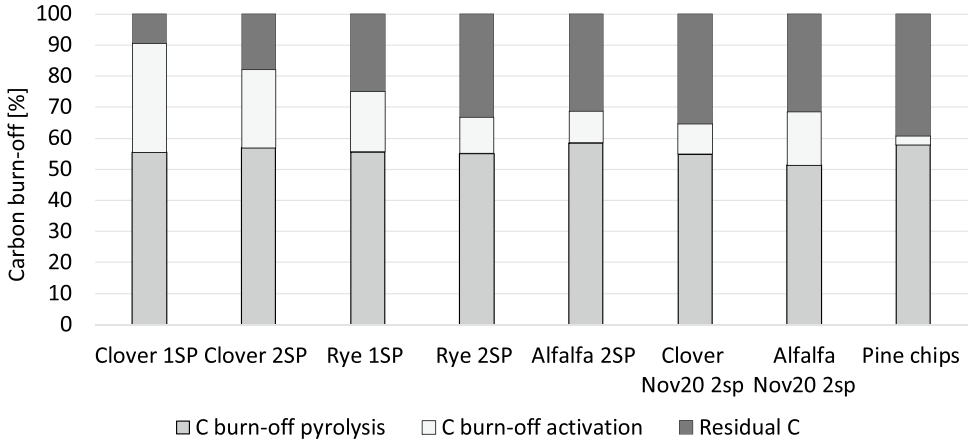

Fig. 4 Carbon burn-off after the pyrolysis and the activation steps, relative to the carbon content of the dry pulp

Figure 4 shows the C burn-off calculated as in Eq. 1 for the different samples after the pyrolysis and after the steam activation step. The C concentrations measured in the samples after drying, pyrolysis, and activation are reported in the supplementary material. The C burn-off during pyrolysis was similar for all the pulp samples (between 50 and 55 wt%), while it varied significantly during the steam activation step. This was most likely a consequence of the different elements present in the ash fraction, that influence the reactivity of each biochar in the presence of steam. Indeed, the C burn-off appeared to be positively correlated with the total ash content in the pulp samples (Fig. 5a), but not in the same way for all elements. The C burn-off appeared to be positively correlated with the content of most elements reported in Table 2. On the other hand, the correlation with the content of Ca appeared uncertain and possibly negative: Fig. 5b shows the correlation between the K and Ca

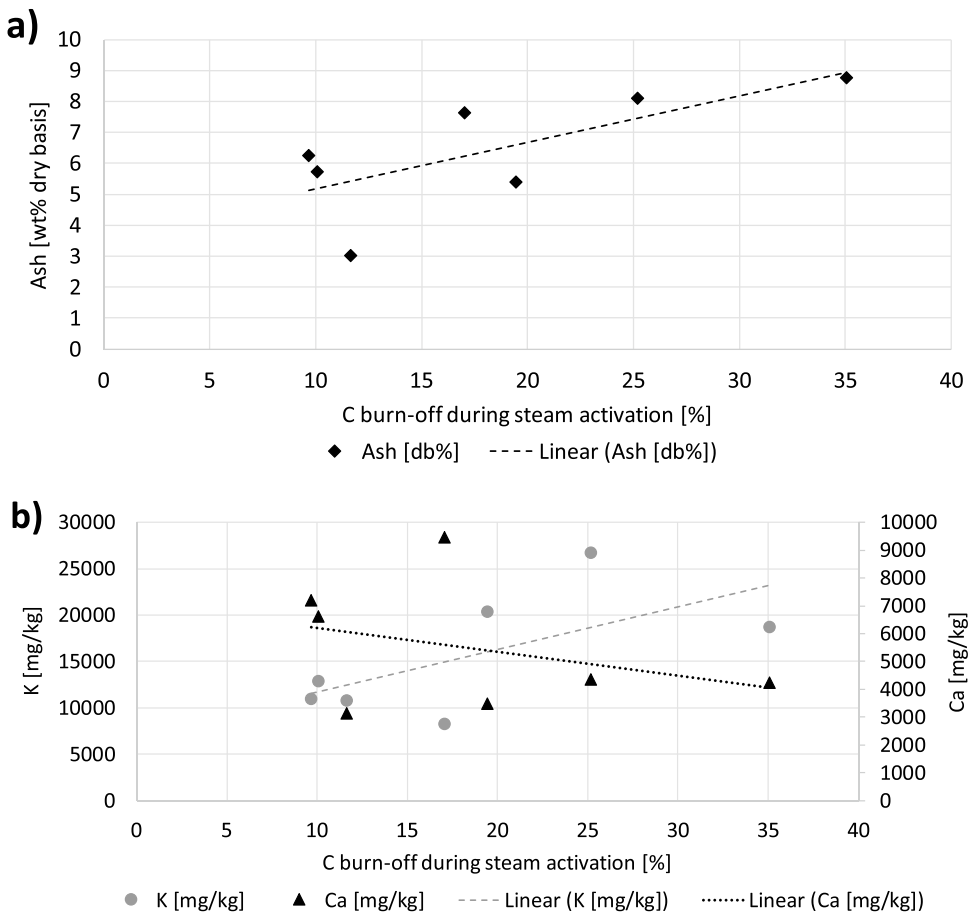

Fig. 5 Correlation of the C burn-off with the total ash content (**a**) and the potassium (K) and calcium (Ca) content of the pulp samples. Linear trend lines are shown for all datasets

content and the C burn-off during activation. Correlations with the content of P, Mg, S, and Si can be found in the supplementary material. Alkali and alkaline earth metals (AAEMs) are known to have a catalytic effect on the gasification of biomass, with K being reported as the most active [52]. Ca, on the other hand, has been found in some cases to exert an inhibitory effect on both steam and CO_2 gasification reactions of biochar [53, 54].

The higher level of C burn-off during activation did not correspond to a larger final surface area. For example, clover (1SP and 2SP) showed the highest C burn-off during steam activation but yielded a lower final surface area compared with the other pulp samples. Interestingly, clover pulp from a later harvest showed a lower C burn-off during activation but a final surface area comparable with early harvested clover. This can be ascribed to a lower content of minerals and higher content of lignin (Tables 1 and 3), consistent with the grass maturation process.

Overall, samples with lower ash and higher lignin content appeared to yield biochars with improved surface area and porosity following steam activation. This result suggests that the best-quality activated biochar can be obtained from double-pressed pulp and from grasses and legumes harvested at higher maturity.

In order to compare the laboratory results with the actual process, the surface area and porosity were also measured on a pulp biochar obtained with the AquaGreen 100 kWth pilot plant. The sample was obtained from clover pulp 2SP, and the maximum temperature reached within the process was 680 °C. The obtained biochar had a specific surface area of 104 m^2/g and a pore volume of 0.0579 cm^3/g. These values are not as high as those obtained after the laboratory steam activation, but they are certainly higher compared with the samples from batch pyrolysis in the same temperature range. This result suggests that the presence of steam in the pyrolysis stage within the AquaGreen system is beneficial for the surface structure of the final biochar product, and might be used to improve the adsorption capability.

3.3 Stability indicators of the carbon fraction of biochars

The H/C ratios for the different biochars are shown in Fig. 6, alongside the recalcitrance ratio R_{50} resulting from the thermogravimetric analysis presented in Sect. 3.1. The H/C ratio for all the pyrolysis samples was in the range 0.28–0.4, while the steam activation had the effect of reducing the H/C ratio for the majority of the samples, suggesting a slightly increased recalcitrance as a consequence of activation. This can be ascribed to the loss of more labile carbon during the steam activation treatment.

For the analyzed samples, the R_{50} value appeared to vary in a narrower range than the H/C ratio. The correlation between the two parameters appeared consistent for the pyrolysis chars, where lower H/C ratios corresponded to higher R_{50} values. The correlation was not as clear for the activated chars: in most cases the H/C ratio was clearly reduced compared to the pyrolysis sample, but R_{50} appeared hardly affected by the activation, if at all. The most significant difference in the R_{50} value was between the pulp and the pine chips biochar, the latter having the highest R_{50} value of 0.57. This result indicates that the temperature at which the carbon oxidizes for the pulp biochars is lower than that of the pine chips biochar; the latter is therefore considered more recalcitrant in the environment.

Overall, the H/C ratio appears more sensitive than R_{50} to changes in the biochar structure due to the activation treatment. According to current indications of the European Biochar Foundation, a biochar is considered to be completely pyrolyzed if the H/C_{org} ratio is < 0.7, which is the prerequisite for EBC certification [16]. Moreover, the carbon stability of biochar for carbon sequestration is considered the highest (a conservative average degradation rate of 0.3% per year) when the $H:C_{org}$ ratio is below 0.4 [13]. Based on the obtained H/C ratios, according to Budai et al. [38] at least 70% of the carbon in the biochar is predicted to be recalcitrant in soil for 100 years, with 95% confidence. In the context of this work, the results indicate that all the pulp biochars have a high theoretical recalcitrance in the

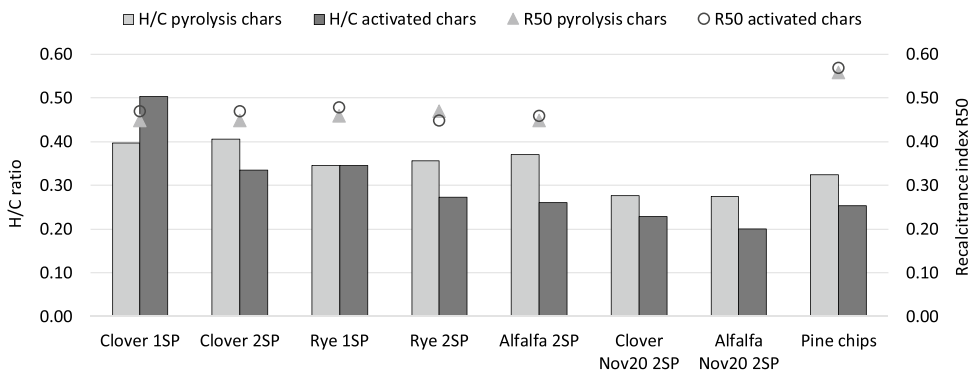

Fig. 6 H/C ratio and recalcitrance index R50 of pyrolysis and steam activated biochars. R_{50} was not measured for Nov20 samples

environment and therefore a good carbon sequestration potential, especially after the activation step. Such potential can be realized if the biochar is used directly as soil amendment or incorporated into soils after its cascade use in animal feed, bedding, composting and similar applications [13].

3.4 Results of mass- and energy balances and assessment of climate crisis mitigation potentials

The main results from the energy and mass balance calculations for a system with integrated char activation are provided in the charts in Figs. 7 and 8, with variation of grass pulp type and sample moisture content. The individual components of the energy balance are summed up — where relevant, of heat capacity, chemical energy potential, and enthalpy of evaporation (steam only). The results can be related to the products illustrated in the system layout (Fig. 1), where product C1 corresponds to the pyrolysis gas, biochar is C3, activation gas is C2, low temperature heat is B2, and low temperature steam is B3.

Figure 7 shows that among different types of pulp, results vary primarily with the level of C burn-off (char gasification) during the activation step. In processes with substantial char gasification, a large fraction of the energy in the char is transferred into the activation gas, consisting mainly of CO and H_2 resulting from the reaction of carbon with steam, as well as residual steam at around 650 °C. In addition, a severe char activation requires additional heat and steam which, in these calculations, reduce the heating potential of the residual pyrolysis gas and the amount of low temperature steam from the dryer. Across the 5 different pulp samples, 4–5% of the energy in the excess pyrolysis gas is found in the form of heat, while 95–96% is in the chemical energy potential/HHV. In the activated biochar product, the split is 5–9% as heat and the rest as HHV while the split in the non-activated biochar fractions contain around 3% energy as heat and 97% as HHV. In the calculations, there is a fixed relationship between heat and evaporation enthalpy (32% of energy) and HHV (68% of energy) in the activation gas, determined by the excess steam ratio. Similarly, there is a fixed ratio between the

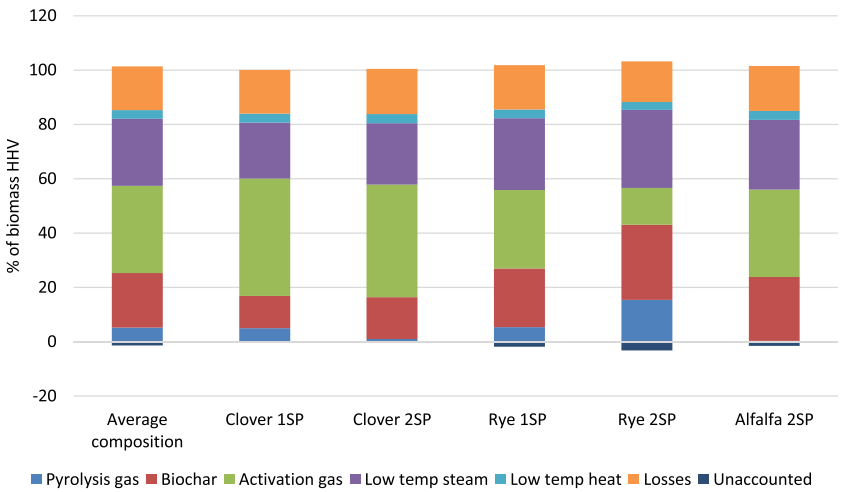

Fig. 7 Energy balance estimation in system with integrated char activation as function of grass pulp sample composition. Average composition of five different pulp types also included. See Fig. 1 for system layout. Pyrolysis gas = C1, activation gas = C2, biochar = C3, low temperature heat = B2, and low-temperature steam = B3

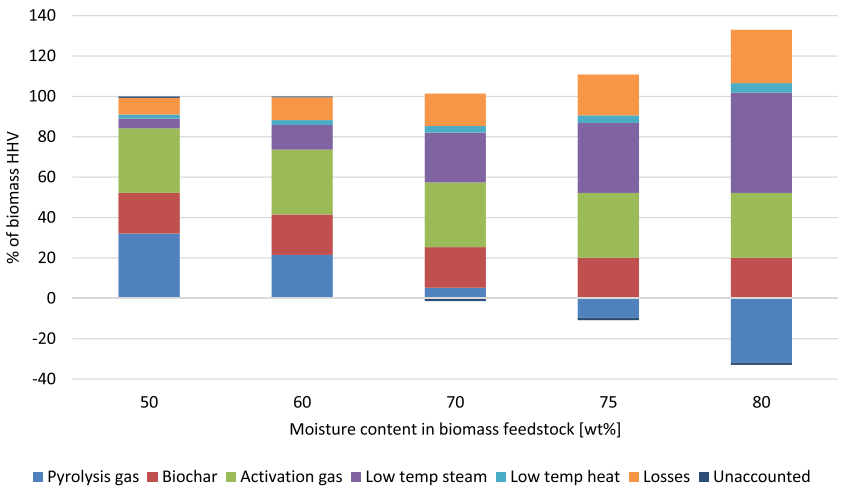

Fig. 8 Energy balance estimation in system with integrated char activation as function of biomass moisture content. Average composition of five different grass pulp types used (data in Table 1, Table 4, and Fig. 4). See Fig. 1 for system layout. Pyrolysis gas = C1, activation gas = C2, biochar = C3, low-temperature heat = B2, and low-temperature steam = B3

amount of energy in the residual steam in the activation gas that can be extracted at high temperatures from 100 to 650 °C (around 30%) and at temperatures below 100 °C via condensation (around 70%). In the subsequent use of the results, all the sensible heat — both high and low temperature, in the gas product from char activation is assumed used for low-temperature purposes in the production of district heating services After cooling and condensation of the steam, the permanent gases can be used for high temperature purposes and advanced uses.

Figure 8 shows uses an average composition across five pulp samples and shows that the moisture content in the fuel should be between 50 and 75 wt% to fulfill the requirements in the current system layout. With the estimated steam-carbon ratio in char activation of 500 molar% steam surplus, at least 45% moisture in the grass pulp substrate is required to provide sufficient steam from the steam dryer to supply enough heat for the char activation process. Similarly, there is a maximum moisture content of around 70–75% in the average grass pulp where after there will be an energy deficit in the system unless unutilized energy potential in the biochar or the residual gas from char activation is exploited. The latter is the main boundary condition as the steam requirement is highly uncertain and there is plenty of energy in the low-moisture system to produce steam from water from the green biorefinery. For systems without char gasification, there is no lower moisture limit, while the upper moisture limit is somewhat higher and found to be around 80 wt% moisture (results not shown).

From the energy- and mass-balance calculations, a product distribution to be used for the climate impact assessment is extracted. This product distribution is provided in Table 6 for five different grass pulp substrates with 70 wt% moisture, in systems with and without steam activation of biochar.

In the assessment of the potential climate impact, based on the H/C ratios measured on the pulp biochars (Fig. 6), and discussed in Sect. 3.3, it is assumed that the carbon sink potential in all chars is 70% of C content. Moreover, the following product uses and effects are assumed:

- Product 1: Biochar and activated biochar is sequestered, with a climate impact of 3.67 kg $CO_{2\text{-eq}}$ per kg C persisting after 100 years, based on BC_{100} stability factors. 3.67 is the mass ratio between 1 mol of CO_2 and 1 mol of carbon. Heat in the biochar is not recovered. There are many possible uses of the biochar products before amendment into soil, such as feed additive, especially if steam-activated. These uses may also have substantial climate impacts, but these are not included in this assessment.
- Products 4, 5, and 7: It is assumed that the energy in these product streams is used either for low-temperature process heat in the adjacent green biorefinery, or for production of district heating. To investigate the different use cases, the effect of products 4, 5, and 7 is modeled substituting either marginal Danish district heating (replacement effect of 10.4 kg $CO_{2\text{-eq}}$ per GJ) or heat from natural gas (replacement effect of 66.0 kg $CO_{2\text{-eq}}$ per GJ).
- Products 2, 3, and 6: These are high energy quality products that can be used for various purposes. In the current study, the use is focused on high temperature process heat, while other options like oil extraction and fuel synthesis may also be both possible and relevant. In the best case, the high-temperature heat is assumed to replace heat from combustion of coal (replacement effect of 112.2 kg $CO_{2\text{-eq}}$ per GJ), while the heat is used for production of marginal district heating in the worst case (replacement effect of 10.4 kg $CO_{2\text{-eq}}$ per GJ).

Table 6 Products and product characteristics from integrated steam drying and thermal pyrolysis of 1 ton grass pulp as received from green biorefinery, with 70 wt% moisture. Results for systems with and without char activation. DH: district heating. HHV: higher heating value

	System with char activation					System without char activation				
	Clover 1SP	Clover 2SP	Rye 1SP	Rye 2SP	Alfalfa 2SP	Clover 1SP	Clover 2SP	Rye 1SP	Rye 2SP	Alfalfa 2SP
Biochar										
kg biochar carbon (1)	20	25	28	42	29	57	59	52	55	55
Excess pyrolysis gas										
GJ process heat (2)	0.01	0.00	0.01	0.04	0.00	0.04	0.04	0.04	0.05	0.03
GJ HHV (3)	0.27	0.05	0.29	0.88	0.02	1.06	0.78	0.80	1.17	0.60
Excess steam from dryer										
GJ DH or similar (4)	1.19	1.25	1.47	1.72	1.41	1.94	1.94	1.95	1.97	1.95
Activation gas										
GJ DH or similar (5)	0.80	0.74	0.52	0.26	0.57	0.00	0.00	0.00	0.00	0.00
GJ HHV (6)	1.69	1.55	1.09	0.55	1.21	0.00	0.00	0.00	0.00	0.00
Low-temperature heat from exhaust and condensate										
GJ DH or similar (7)	0.19	0.19	0.18	0.17	0.18	0.17	0.17	0.16	0.16	0.16

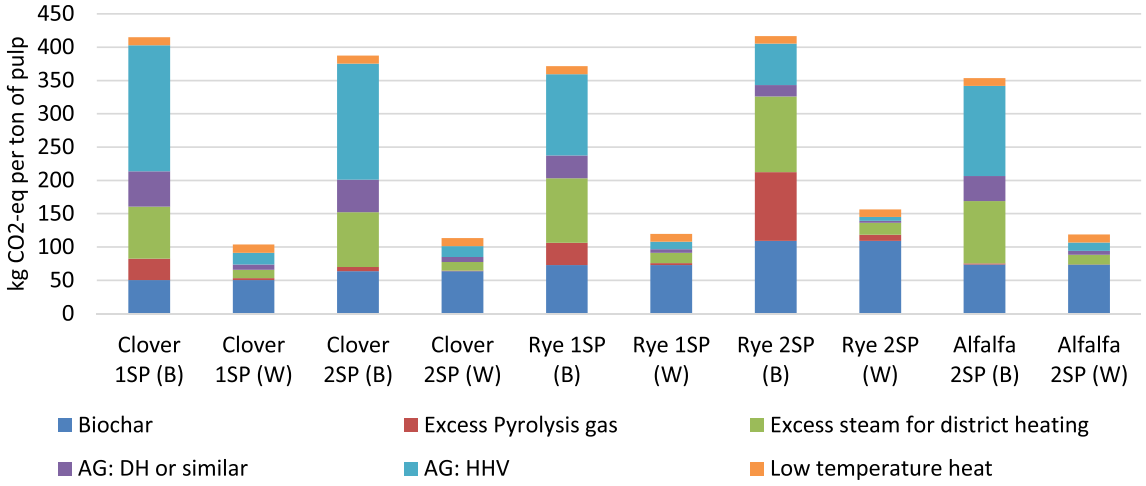

Fig. 9 Best and worst case potential climate crisis mitigation value of products from steam drying and thermal pyrolysis of various grass pulp samples (70 wt% moisture) in a system with steam char activation. Results per ton of pulp with 70 wt% moisture. AG, residual activation gas; DH, district heating; HHV, higher heating value; B, best case; W, worst case

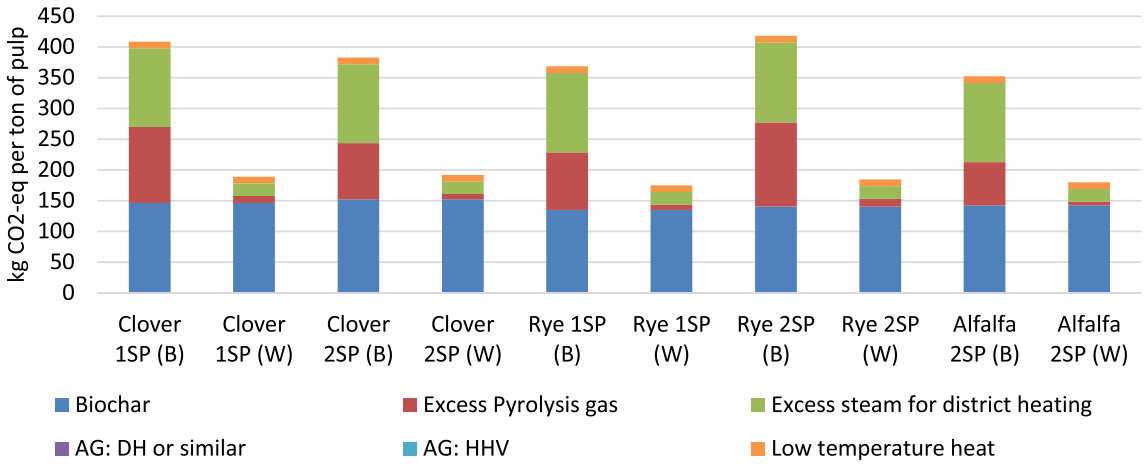

Fig. 10 Best- and worst-case potential climate crisis mitigation value of products from steam drying and thermal pyrolysis of various grass pulp samples (70 wt% moisture) in a system without steam char activation. Results per ton of pulp with 70 wt% moisture. AG, residual activation gas; DH, district heating; HHV, higher heating value; B, best case; W, worst case

From the assessment results reported in Figs. 9 and 10, it is evident that the end-use of energy-products from the proposed system has a huge impact on the potential climate crisis mitigation effect. This is especially evident in the system with char activation where there is a difference between the best and worst case of a factor of 3–4. In the system without char activation, the biochar plays a large role in the final result, which stabilize the impact potential across the energy product end-use scenarios. In this system, the difference between the best and worst case setting is around a factor of 2.

The difference in the total effect of the systems with and without char activation is insignificant in the best case scenarios (minimum impact is 0–2% lower than maximum impact), while it is substantially higher in the worst-case scenarios where the climate mitigation potentials of the products from the system with char activation is 15–45% lower than the potentials related to the systems without char activation.

The influence of moisture content of the grass pulp substrate has also been assessed. Results from the system with char activation are presented in Fig. 11. Calculations are made per ton of dry matter of pulp feedstock, with moisture content varying from 50 to 70 wt%. These moisture levels were determined as soft boundary conditions in the energy and mass balance calculations, as feasible for the operation of a system with char activation without external supply of steam or heat.

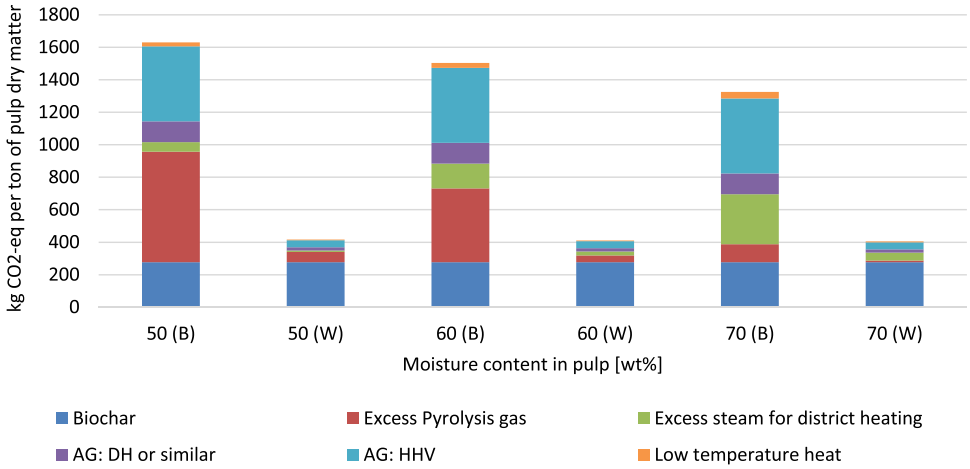

Fig. 11 Best- and worst-case potential climate crisis mitigation value of products from steam drying and thermal pyrolysis of an average composition grass pulp sample (average of five different samples) as function of moisture content from 50 to 70 wt% in a system with steam char activation. Calculation per ton dry matter. AG, residual activation gas; DH, district heating; HHV, higher heating value; B, best case; W, worst case

From these results, it is evident that under worst case conditions, the influence of moisture content on the climate mitigation potential of the products is not significant. Under worst-case conditions, it is the biochar carbon sequestration effect that drives the impact potential, regardless of the moisture content, at least as long as there is sufficient energy to avoid exploitation of biochar carbon for energy purposes. Under best-case conditions, there is a steady decline in mitigation potential with increasing moisture content. This development is largely based on the shift from coal-substitution to natural gas substitution, which has a much smaller climate intensity.

In addition, from the assessment of systems without char activation (results provided in supplementary material), it is found that the mitigation potential of systems with char activation is much more dependent on the value of the energy-use than in systems without char activation. Increased focus on the value of the energy product increases the uncertainty and sensitivity related to the climate benefit, and makes it more vulnerable to a continuous sustainable transition in the surrounding energy system [40]. This should be given a very high priority during planning, implementation, and operation of such systems.

Overall, it is found that biochar activation can influence the climate impact of grass pulp pyrolysis, but also that circumstances related to use of energy products, and particularly the residual activation gas, may play a substantial part in the final accounting. From the results reported in this work regarding the structural and composition changes during char activation, it is likely that the activation step may foster a high value biochar utilization (e.g., as feed additive) and that its cascade use may induce additional climate benefits. However, the price to pay is a carbon loss affecting the biochar C-sink potential as well as a different set of circumstances related to the production and use of energy products.

The assessment of the climate mitigation impact is based on relatively simple energy and mass balances and contains some sensitive assumptions and parameters. There could be many other energy-product use situations as well as variations in feedstock composition and system layout. For example, in situations with small plants with low thermal capacities or limited end-use options, it may not be economically feasible to optimize use of all energy products. In such cases, it could become viable to gather all energy streams for a single use, e.g., as local supply or for a district heating network. In single-use cases, the potential climate crisis mitigation potential will depend heavily on the climate intensity of the energy source substituted. In addition, there are some central omitted aspects that should be addressed in full with a footprint accounting or LCA studies to support or challenge the present results. These include e.g.:

- Effect of biochar in downstream use systems, e.g., as feed additive, filter substrate, etc. This could also be cascade systems and the effects on the fate in soil should also be included.
- Effect of increased transportation input and utilities for system modification (drying, pyrolysis, and char activation) — however, this has previously been found to have limited effect on systems for biomass pyrolysis [40]
- The current use of the grass pulp has not been included in the assessment. This is a limitation as the net effect of the proposed system should be calculated as the difference between the effect of the current use and the proposed scenario. If the current use has a climate impact, then this would increase the net effect of the proposed system; in contrast, if the current use provides a climate benefit, then this would reduce the potential net benefit of the proposed system.

4 Conclusions

The integration of a biochar production system in a green biorefinery was investigated with laboratory-scale pyrolysis and biochar characterization, as well as energy and

mass balances to assess the feasibility and the potential climate impact of the integrated system. The residue of green juice extraction, the fiber-rich pulp, was obtained from processing of different grass and legume species with different extraction steps (1 or 2) and with different levels of maturity at harvest. The different types of pulp showed very similar proximate composition and a similar behavior during pyrolysis, yielding biochars with a relatively high carbon content (above 60 wt%), but very low specific surface area and pore volume. Surface area was not improved by increasing the pyrolysis temperature. In contrast, an additional steam activation treatment at 650 °C had a dramatic effect on the surface area of the biochar samples, which increased up to 400 m^2/g. However, pulp samples behaved differently in the activation step, due to their diverse content and composition of inorganics. The results highlighted the importance of the activation step in order to obtain porous pulp biochars with a good potential to be used as animal feed additives. In this regard, highest specific surface area with lower carbon burn-off appeared to be achieved either with pulp that underwent a double pressing, or from pulp samples derived from grasses harvested at higher maturity (with decreased content of inorganics and increased content of lignin). The evaluation of the theoretical carbon stability of the pulp biochars indicated a good carbon sequestration potential for all of them, which might improve after the steam activation treatment. The techno-environmental assessment of the potential climate impact from energy production and carbon sink effects reveals that there are both substantial potential benefits and large variation among the results. The variation is fostered primarily by the end-use of the produced energy products and the related substitution value hereof; therefore, this should be taken into account during planning and implementation. Variation induced by grass pulp characteristics are less significant, except for moisture content which is found to have significant influence on the results as well. The best-case results are found to be comparable in systems with and without char activation, while-worst case results are found to be better in systems without char activation due to the robust effects of biochar carbon storage related to the increased amount of carbon in the biochar. The analysis has identified several key aspects that should be further investigated. The char activation process should be modeled in a situated case context where the process is optimized towards a specific char end-use and use of the activation gas. Moreover, reference grass pulp use effects should be investigated and included in the assessment. Future work should include a complete climate footprint assessment of integrated grass bio-refineries and pyrolysis systems, with and without char activation, preferably based on data from pilot-scale experimental campaigns.

Supplementary Information The online version contains supplementary material available at https://doi.org/10.1007/s13399-023-04877-4.

Acknowledgements The authors would like to thank Malgorzata Rizzi (DTU Environment) for the support with ICP-OES analyses.

Author contribution G. Ravenni: conceptualization, methodology, investigation, data curation, validation, visualization, writing—original draft, writing—review and editing. T. P. Thomsen: conceptualization, methodology, formal analysis, data curation, visualization, writing—original draft. A. M. Smith: conceptualization, investigation, data curation, visualization, writing—original draft. M. A. Jensen: resources, writing—review and editing K.T. Rohde Nielsen: conceptualization, resources. Ulrik B. Henriksen: conceptualization, methodology, supervision.

Funding Open access funding provided by Technical University of Denmark This work was supported by the Ministry of Environment and Food of Denmark, through the Green Development- and Demonstration Program (GUDP), as part of the project "Grass Biochar – energi fra pressepulp fra græsproteinproduktion til drift af raffineringsprocessen og produktion af værdifuldt biokul" with grant number 34009–19-1598.

Data availability Original data for this work are available upon request to the authors.

Declarations

Ethics approval Declaration not applicable.

Competing interests The authors declare the following financial interests/personal relationships which may be considered as potential competing interests: The drying and pyrolysis units mentioned in this work are currently patent pending on behalf of DTU and AquaGreen ApS.

References

1. Santamaria-Fernandez M, Ambye-Jensen M, Damborg VK, Lübeck M (2019) Demonstration-scale protein recovery by lactic acid fermentation from grass clover — a single case of the production of protein concentrate and press cake silage for animal feeding trials. Biofuels, Bioprod Biorefin 13:502–513. https://doi.org/10.1002/bbb.1957
2. Larsen SU, Ambye-Jensen M, Jørgensen H, Jørgensen U (2019) Ensiling of the pulp fraction after biorefining of grass into pulp and protein juice. Indust Crops Prod 139:111576. https://doi.org/10.1016/j.indcrop.2019.111576

3. Chen J, Lærke PE, Jørgensen U (2022) Land conversion from annual to perennial crops: a win-win strategy for biomass yield and soil organic carbon and total nitrogen sequestration, Agriculture. Ecosyst Environ 330:107907. https://doi.org/10.1016/j.agee.2022.107907
4. Behazin E, Ogunsona E, Rodriguez-Uribe A, Mohanty AK, Misra M, Anyia AO (2016) Mechanical, chemical, and physical properties of wood and perennial grass biochars for possible composite application. BioResourc 11:1334–1348
5. Trippe KM, Griffith SM, Banowetz GM, Whitaker GW (2015) Changes in soil chemistry following wood and grass biochar amendments to an acidic agricultural production soil. Agron J 107:1440–1446. https://doi.org/10.2134/agronj14.0593
6. O Mašek (2016) Biochar in thermal and thermochemical biorefineries-production of biochar as a coproduct, in: Handbook of biofuels production: processes and technologies: Second Edition, Elsevier - Woodhead Publishing, 655–671. https://doi.org/10.1016/B978-0-08-100455-5.00021-7.
7. M Puig-Arnavat, TP Thomsen, Z Sárossy, RØ Gadsbøll, LR Clausen, J Ahrenfeldt (2020) Biomass gasification for bioenergy, in: C. Saffron (Ed.), Achieving carbon negative bioenergy systems from plant materials, Burleigh Dodds Science Publishing Limited, 19–58. https://doi.org/10.1201/9781003047612.
8. Panahi HK, Dehhaghi M, Ok YS, Nizami AS, Khoshnevisan B, Mussatto SI, Aghbashlo M, Tabatabaei M, Lam SS (2020) A comprehensive review of engineered biochar: production, characteristics, and environmental applications. J Clean Prod 270:122462. https://doi.org/10.1016/j.jclepro.2020.122462
9. Sanchez-Monedero MA, Cayuela ML, Roig A, Jindo K, Mondini C, Bolan N (2018) Role of biochar as an additive in organic waste composting. Biores Technol 247:1155–1164. https://doi.org/10.1016/j.biortech.2017.09.193
10. Chiappero M, Norouzi O, Hu M, Demichelis F, Berruti F, Di Maria F, Mašek OS (2020) Fiore, Review of biochar role as additive in anaerobic digestion processes. Renew Sustain Energy Rev 131:110037. https://doi.org/10.1016/j.rser.2020.110037
11. Schmidt HP, Hagemann N, Draper K, Kammann C (2019) The use of biochar in animal feeding. PeerJ 2019:1–54. https://doi.org/10.7717/peerj.7373
12. Man KY, Chow KL, Man YB, Mo WY, Wong MH (2020) Use of biochar as feed supplements for animal farming. Critical Reviews in Environmental Science and Technology. 1–31. https://doi.org/10.1080/10643389.2020.1721980.
13. European Biochar Certificate (EBC) Certification of the carbon sink potential of biochar, Ithaka Institute, Arbaz, Switzerland. Version 2.1E of 1st February 2021. https://www.european-biochar.org/media/doc/2/c_en_sink-value_2-1.pdf. Accessed 20 Sept 23
14. Schmidt HP, Anca-Couce A, Hagemann N, Werner C, Gerten D, Lucht W, Kammann C (2019) Pyrogenic carbon capture and storage. GCB Bioenergy 11:573–591. https://doi.org/10.1111/gcbb.12553
15. European Commission (2011) Commission Regulation No 575/2011 on the Catalogue of feed materials. https://eur-lex.europa.eu/LexUriServ/LexUriServ.do?uri=OJ:L:2011:159:0025:0065:en:PDF. Accessed 20 Sept 23
16. European Biochar Foundation. Biochar for use as animal feed additive – chapter 9 of the European Biochar Certificate (EBC), Arbaz, Switzerland. Version 9.2E of 2nd December 2020. https://european-biochar.org. Accessed 20 Sept 23
17. Ioannidou O, Zabaniotou A (2007) Agricultural residues as precursors for activated carbon production—a review. Renew Sustain Energy Rev 11:1966–2005. https://doi.org/10.1016/j.rser.2006.03.013
18. Chen Y, Zhu Y, Wang Z, Li Y, Wang L, Ding L, Gao X, Ma Y, Guo Y (2011) Application studies of activated carbon derived from rice husks produced by chemical-thermal process — a review. Adv Coll Interface Sci 163:39–52. https://doi.org/10.1016/j.cis.2011.01.006
19. Joseph B, Kaetzl K, Hensgen F, Schäfer B, Wachendorf M (2020) Sustainability assessment of activated carbon from residual biomass used for micropollutant removal at a full-scale wastewater treatment plant. Environ Res Lett 15(6):064023. https://doi.org/10.1088/1748-9326/ab8330
20. Molina-Sabio M, González MT, Rodriguez-Reinoso F, Sepúlveda-Escribano A (1996) Effect of steam and carbon dioxide activation in the micropore size distribution of activated carbon. Carbon 34:505–509. https://doi.org/10.1016/0008-6223(96)00006-1
21. Tomków K, Siemieniewska T, Czechowski F, Jankowska A (1977) Formation of porous structures in activated brown-coal chars using O_2, CO_2 and H_2O as activating agents. Fuel 56:121–124
22. Galvano F, Pietri A, Bertuzzi T, Bognanno M, Chies L, De Angelis A, Galvano M (1997) Activated carbons: in vitro affinity for fumonisin B1 and relation of adsorption ability to physicochemical parameters. J Food Prot 60:985–991. https://doi.org/10.4315/0362-028X-60.8.985
23. Edrington TS, Kubena LF, Harvey RB, Rottinghaus GE (1997) Influence of a superactivated charcoal on the toxic effects of aflatoxin or T-2 toxin in growing broilers. Poult Sci 76:1205–1211. https://doi.org/10.1093/ps/76.9.1205
24. Djomo SN, Knudsen MT, Martinsen L, Andersen MS, Ambye-Jensen M, Møller HB, Hermansen JE (2020) Green proteins: an energy-efficient solution for increased self-sufficiency in protein in Europe. Biofuels, Bioprod Biorefin 14:605–619. https://doi.org/10.1002/bbb.2098
25. Pape T, Ahrenfeldt J, Tjalfe S, Thomsen TPTP, Ahrenfeldt J, Thomsen STST, Pape T, Ahrenfeldt J, Tjalfe S, Thomsen TPTP, Ahrenfeldt J, Thomsen STST (2013) Assessment of a novel alder biorefinery concept to meet demands of economic feasibility, energy production and long term environmental sustainability. Biomass Bioenerg 53:81–94. https://doi.org/10.1016/j.biombioe.2013.02.022
26. Corona A, Parajuli R, Ambye-Jensen M, Hauschild MZ, Birkved M (2018) Environmental screening of potential biomass for green biorefinery conversion. J Clean Prod 189:344–357. https://doi.org/10.1016/j.jclepro.2018.03.316
27. Corona A, Ambye-Jensen M, Vega GC, Hauschild MZ, Birkved M (2018) Techno-environmental assessment of the green biorefinery concept: combining process simulation and life cycle assessment at an early design stage. Sci Total Environ 635:100–111. https://doi.org/10.1016/j.scitotenv.2018.03.357
28. M Puig-Arnavat, TP Thomsen, G Ravenni, LR Clausen, Z Sárossy, J Ahrenfeldt, Pyrolysis and Gasification of Lignocellulosic Biomass, in: J.R. Bastidas-Oyanedel, J.E. Schmidt (Eds.), Biorefinery, Springer Nature Switzerland AG, 2019: 79–110. https://doi.org/10.1007/978-3-030-10961-5_4.
29. Clausen LRLR (2017) Energy efficient thermochemical conversion of very wet biomass to biofuels by integration of steam drying, steam electrolysis and gasification. Energy 125:327–336. https://doi.org/10.1016/j.energy.2017.02.132
30. Harvey OR, Kuo LJ, Zimmerman AR, Louchouarn P, Amonette JE, Herbert BE (2012) An index-based approach to assessing recalcitrance and soil carbon sequestration potential of engineered black carbons (biochars). Environ Sci Technol 46:1415–1421. https://doi.org/10.1021/es2040398
31. Liu X, Chang F, Wang C, Jin Z, Wu J, Zuo J, Wang K (2018) Pyrolysis and subsequent direct combustion of pyrolytic gases for sewage sludge treatment in China. Appl Therm Eng 128:464–470. https://doi.org/10.1016/j.applthermaleng.2017.08.091

32. Engineeringtoolbox.com, The Engineering ToolBox - Water Vapor - Specific Heat (2016) https://www.engineeringtoolbox.com/water-vapor-d_979.html. Accessed 20 Sept 23
33. Engineeringtoolbox.com, The Engineering ToolBox - Solids - Specific Heats (2016) https://www.engineeringtoolbox.com/specific-heat-solids-d_154.html. Accessed 20 Sept 23
34. Engineeringtoolbox.com, Specific Heat of some Liquids and Fluids (2003) https://www.engineeringtoolbox.com/specific-heat-fluids-d_151.html. Accessed 20 Sept 23
35. P. Datt (2011) Latent heat of vaporization/condensation, Springer Science+Business Media B.V. https://doi.org/10.1007/978-90-481-2642-2.
36. Ding H-S, Jiang H (2013) Self-heating co-pyrolysis of excessive activated sludge with waste biomass: energy balance and sludge reduction. Biores Technol 133:16–22. https://doi.org/10.1016/j.biortech.2013.01.090
37. P. Basu (2018) Chapter 7 - Gasification Theory, in: Biomass gasification, pyrolysis and torrefaction — practical design and theory, Third, Academic Press, 2018: 211–262. https://doi.org/10.1016/B978-0-12-812992-0.00007-8.
38. Budai A, Zimmerman AR, Cowie AL, Webber JB, Singh BP, Glaser B, Masiello CA, Andersson D, Shields F, Lehmann J, Camps Arbestain M, Williams M, Sohi M, Joseph S (2013) Biochar carbon stability test method: an assessment of methods to determine biochar carbon stability. International Biochar Initiative. September 20, 2013. https://biochar-international.org/wp-content/uploads/2018/06/IBI_Report_Biochar_Stability_Test_Method_Final.pdf. Accessed 20 Sept 23
39. The Netherlands Enterprise Agency (RVO), BioGrace II, Online Database and Modelling Tool (2018) https://www.biograce.net/biograce2/. Accessed 20 Sept 23
40. Thomsen TP (2021) Climate footprint analysis of straw pyrolysis & straw biogas — assessment of the Danish climate crisis mitigation potential of two new straw management options. Roskilde, Denmark
41. Muñoz I, Weidema BP (2021) Example — marginal electricity in Denmark. Version: 2021–06–08. https://www.consequential-lca.org. Accessed 20 Sept 2023
42. Ecoinvent, Ecoinvent Consequential Database 3.7.1. (2020) https://ecoquery.ecoinvent.org/3.7.1/consequential/search. Accessed 20 Sept 23
43. Turconi R, Tonini D, Nielsen CFB, Simonsen CG, Astrup T (2014) Environmental impacts of future low-carbon electricity systems: detailed life cycle assessment of a Danish case study. Appl Energy 132:66–73. https://doi.org/10.1016/j.apenergy.2014.06.078
44. Demirbaş A (2003) Relationships between lignin contents and fixed carbon contents of biomass samples. Energy Convers Manage 44:1481–1486. https://doi.org/10.1016/S0196-8904(02)00168-1
45. Bin Kim H, Kim JG, Kim T, Alessi DS, Baek K (2020) Mobility of arsenic in soil amended with biochar derived from biomass with different lignin contents: relationships between lignin content and dissolved organic matter leaching. Chem Eng J 393:124687. https://doi.org/10.1016/j.cej.2020.124687
46. Ippolito JA, Cui L, Kammann C, Wrage-Mönnig N, Estavillo JM, Fuertes-Mendizabal T, Cayuela ML, Sigua G, Novak J, Spokas K, Borchard N (2020) Feedstock choice, pyrolysis temperature and type influence biochar characteristics: a comprehensive meta-data analysis review. Biochar 2:421–438. https://doi.org/10.1007/s42773-020-00067-x
47. Ferraro G, Pecori G, Rosi L, Bettucci L, Fratini E, Casini D, Rizzo AM, Chiaramonti D (2021) Biochar from lab-scale pyrolysis: influence of feedstock and operational temperature. Biomass Convers Biorefinery. https://doi.org/10.1007/s13399-021-01303-5
48. Weber K, Quicker P (2018) Properties of biochar. Fuel 217:240–261. https://doi.org/10.1016/j.fuel.2017.12.054
49. Fu P, Hu S, Xiang J, Sun L, Li P, Zhang J, Zheng C (2009) Pyrolysis of maize stalk on the characterization of chars formed under different devolatilization conditions. Energy Fuels 23:4605–4611. https://doi.org/10.1021/ef900268y
50. Burhenne L, Damiani M, Aicher T (2013) Effect of feedstock water content and pyrolysis temperature on the structure and reactivity of spruce wood char produced in fixed bed pyrolysis. Fuel 107:836–847. https://doi.org/10.1016/j.fuel.2013.01.033
51. Korus A, Gutierrez JP, Szlęk A, Jagiello J, Hornung A (2022) Pore development during CO_2 and H_2O activation associated with the catalytic role of inherent inorganics in sewage sludge char and its performance during the reforming of volatiles. Chem Eng J 446:137298. https://doi.org/10.1016/j.cej.2022.137298
52. Dahou T, Defoort F, Khiari B, Labaki M, Dupont C, Jeguirim M (2021) Role of inorganics on the biomass char gasification reactivity: a review involving reaction mechanisms and kinetics models. Renew Sustain Energy Rev 135:110136. https://doi.org/10.1016/j.rser.2020.110136
53. González-Vázquez MP, García R, Gil MV, Pevida C, Rubiera F (2018) Unconventional biomass fuels for steam gasification: kinetic analysis and effect of ash composition on reactivity. Energy 155:426–437. https://doi.org/10.1016/j.energy.2018.04.188
54. Bennici S, Jeguirim M, Limousy L, Haddad K, Vaulot C, Michelin L, Zorpas AA (2019) Influence of CO_2 concentration and inorganic species on the gasification of lignocellulosic biomass derived chars. Waste Biomass Valorization. 10:3745–3752. https://doi.org/10.1007/s12649-019-00658-1